Hampered long-term depression and thin spine loss in the nucleus accumbens of ethanol-dependent rats

Saturnino Spiga[a,1], Giuseppe Talani[b,1], Giovanna Mulas[a,c], Valentina Licheri[a], Giulia R. Fois[d], Giulia Muggironi[d], Nicola Masala[a], Carla Cannizzaro[c], Giovanni Biggio[a,b], Enrico Sanna[a,b], and Marco Diana[d,2]

[a]Department of Life and Environmental Sciences, University of Cagliari, 09126 Cagliari, Italy; [b]Institute of Neuroscience, National Research Council, Monserrato, 09042 Cagliari, Italy; [c]Department of Sciences for Health Promotion, University of Palermo, 90127 Palermo, Italy; and [d]"G. Minardi" Laboratory of Cognitive Neuroscience, Department of Chemistry and Pharmacy, University of Sassari, 07100 Sassari, Italy

Edited by Roberto Malinow, University of California, San Diego, La Jolla, CA, and approved July 23, 2014 (received for review April 15, 2014)

Alcoholism involves long-term cognitive deficits, including memory impairment, resulting in substantial cost to society. Neuronal refinement and stabilization are hypothesized to confer resilience to poor decision making and addictive-like behaviors, such as excessive ethanol drinking and dependence. Accordingly, structural abnormalities are likely to contribute to synaptic dysfunctions that occur from suddenly ceasing the use of alcohol after chronic ingestion. Here we show that ethanol-dependent rats display a loss of dendritic spines in medium spiny neurons of the nucleus accumbens (Nacc) shell, accompanied by a reduction of tyrosine hydroxylase immunostaining and postsynaptic density 95-positive elements. Further analysis indicates that "long thin" but not "mushroom" spines are selectively affected. In addition, patch-clamp experiments from Nacc slices reveal that long-term depression (LTD) formation is hampered, with parallel changes in field potential recordings and reductions in NMDA-mediated synaptic currents. These changes are restricted to the withdrawal phase of ethanol dependence, suggesting their relevance in the genesis of signs and/or symptoms affecting ethanol withdrawal and thus the whole addictive cycle. Overall, these results highlight the key role of dynamic alterations in dendritic spines and their presynaptic afferents in the evolution of alcohol dependence. Furthermore, they suggest that the selective loss of long thin spines together with a reduced NMDA receptor function may affect learning. Disruption of this LTD could contribute to the rigid emotional and motivational state observed in alcohol dependence.

dopamine | synaptic plasticity | Golgi | glutamate

Alcohol addiction is a major public health problem in the Western world. In the United States alone, about 15% of adults have an alcohol-related disorder at some point in their life, and alcohol abuse costs the economy over $220 billion per y in medical care and productivity loss (1). A general consensus has emerged on drug addiction as a substance-induced, aberrant form of neural plasticity (2, 3). The nucleus accumbens (Nacc) plays a central role in the neural circuits that are responsible for goal-directed behaviors (4, 5) and in addictive states. Its activity is heavily modulated by glutamate- (GLU) and dopamine- (DA) containing projections that originate in cortical and limbic regions and converge on a common postsynaptic target: the medium spiny neuron (MSN). Furthermore, DA modulates GLU inputs to Nacc neurons (6, 7), both by directly influencing synaptic transmission and by modulating voltage-dependent conductances (8). Accordingly, interactions between DA and GLU are involved in drug-induced locomotor stimulation and addiction (9, 10) and may represent useful potential therapeutic targets (11, 12). In the distal portion of the dendrites of MSNs a significant subpopulation of spines shows a particular synaptic architecture, called the "striatal microcircuit" or "synaptic triad" (13, 14), which is characterized by a double, discrete, and reciprocal interaction between DA and GLU afferents: The former establishes synaptic contact on the spine neck, whereas the latter reaches the head (13). This classical, widely accepted picture has been integrated with the coexistence of DA and GLU on the same neurons (15), but because this phenomenon appears to regress with growth in vitro (16) and its role is unclear at present (17), in the present study GLU and DA will be considered as originating from cortex and ventral tegmental area (VTA), respectively.

At present, little information is available concerning the effects produced by ethanol withdrawal in dependent rats (18), although a selective increase in the density of mushroom-type spines following chronic intermittent ethanol intake has recently been reported on the basal dendrites of layer V neurons of the rodent prefrontal cortex (19). In addition, reduced expression of tyrosine hydroxylase (TH) has been demonstrated in the ventral striatum of rats maintained on a chronic ethanol-containing diet (20), and a decrease of neurofilament protein immunoreactivity in the VTA (21) has been reported. Thus, in the present work, we sought to investigate possible alterations produced by ethanol withdrawal on mesocorticolimbic transmission by exploring critical elements whose presence is strictly correlated with DAergic and GLUergic function, respectively: TH- and dopamine transporter (DAT)-positive fibers and postsynaptic density 95 (PSD-95). Spine density, morphology, and morphometry of MSNs in the Nacc shell were also investigated to obtain structural insights into pre- and postsynaptic elements of the triad simultaneously. Although considered impossible until recently (22), we have developed a new method (23) that allows visualizing the finest morphological details of spinous neurons (Golgi-Cox staining) together with the immunofluorescent neuronal elements under study. By exploiting this novel approach, we are able to visualize

Significance

This paper examines the intimate neuroarchitecture of the nucleus accumbens shell region and how it affects synaptic plasticity in alcohol-dependent rats. To do so, a simultaneous morphometrical/immunofluorescence method was applied to visualize various types of dendritic spines and patch-clamp techniques to detect changes in synaptic currents. Using these tools, we show a selective loss of "long thin" spines accompanied by an impaired long-term depression (LTD) in alcohol-dependent rats. Dopaminergic and glutamatergic signaling are similarly altered. The results highlight the role of long thin dendritic spines in the genesis of LTD in alcohol dependence.

Author contributions: E.S. and M.D. designed research; S.S., G.T., G. Mulas, V.L., G.R.F., G. Muggironi, and N.M. performed research; C.C. and G.B. contributed new reagents/analytic tools; S.S., G.T., E.S., and M.D. analyzed data; and S.S., G.T., E.S., and M.D. wrote the paper.

The authors declare no conflict of interest.

This article is a PNAS Direct Submission.

Freely available online through the PNAS open access option.

[1]S.S. and G.T. contributed equally to this work.

[2]To whom correspondence should be addressed. Email: dsfdiana@uniss.it.

This article contains supporting information online at www.pnas.org/lookup/suppl/doi:10.1073/pnas.1406768111/-/DCSupplemental.

(in the same slice) spine morphology, TH- and DAT-positive fibers, and PSD-95–positive elements to gather information on DA and GLU transmission. Notably, because recent work suggests (24, 25) a potential relationship between spine shape, synaptic function, and morphological rearrangements of the spines as forms of developmental or experience-dependent plasticity (26), we performed patch-clamp experiments in Nacc shell slices obtained from ethanol-withdrawn rats to evaluate whether long-term depression (LTD) formation and its underlying synaptic currents are modified by experimental conditions.

Results

Rats fed on an isocaloric ethanol (EtOH)-containing diet for 20 d were evaluated behaviorally and assigned to experimental groups on the basis of objective withdrawal signs (Fig. S1). Subsequently, all rats were subjected to anatomical or electrophysiological analysis.

Classification of Spines. We classified spine typology using the following morphological/metric criteria (Fig. 1).

Stubby spines. Head diameter almost equal to neck diameter (no distinguishable head) and total length less than 1 μm.

Mushroom spines. Head diameter greater than the maximum diameter of the neck (well-formed head) and neck diameter greater than its length.

Long thin spines. Head diameter greater than the maximum diameter of the neck (well-formed head) and neck length greater than its diameter.

Filopodia. Head diameter almost equal to neck diameter (no distinguishable head) and total length greater than 1 μm.

Spine Density, TH, DAT, and PSD-95 Immunoreactivity Counts. The simultaneous visualization of TH-positive terminals, DAT immunoreactivity, PSD-95–positive antigens, and impregnated MSNs allowed us to study the qualitative and quantitative relationships between these elements. TH-positive fibers mostly engaged putative contacts with the neck of dendritic spines and shafts of MSNs, as expected (13) (Fig. 2*A*). The colocalization between PSD-95– and Golgi-Cox–stained MSNs was found largely on the head of long thin and mushroom (Fig. 2*B*) spines, which were classified morphometrically (Fig. 2*C*) in the three experimental conditions (Fig. 2 and Fig. S2).

As shown in Fig. 3, total spine density on MSN secondary dendritic trunks was found to be significantly different between experimental groups ($F_{119} = 10.01$; $P < 0.0001$). Post hoc analysis showed a selective reduction in spine density in ethanol withdrawal (EtOH-W) ($t_{78} = 3.52$; $P = 0.0007$) but not in chronically ethanol-treated (EtOH-CHR) vs. control (CTRL)-treated rats ($t_{78} = 0.612$; $P = 0.54$). Further, confocal analysis of Golgi-Cox–stained material revealed that long thin spines are the most common spines in CTRL MSNs, representing over 52% of the total (Fig. 3), whereas short (<1-μm) stubby spines reach 27.2%, mushroom-shaped spines reach 11.8%, and filopodia reach 8.9% of all spines detected (Fig. 3). Withdrawal from chronic ethanol produces a decrease of 38.9% in long thin spines only ($F_{118} = 13.3$; $P < 0.0001$), and post hoc analysis disclosed a selective reduction in spine density in EtOH-W compared with CTRL rats ($t = 4.78$; $P < 0.0001$) (Figs. 3 and 4). Further, no statistical differences were found in stubby ($F_{118} = 2.33$; $P = 0.1$), mushroom ($F_{118} = 0.73$; $P = 0.48$), and filopodia ($F_{118} = 0.48$; $P = 0.61$) spine density among treated groups.

As shown in Fig. 4 and Fig. S3, we found that the levels of both TH-positive fibers and PSD-95 decreased by ∼50.7% and ∼61.2%, respectively, in EtOH-W vs. CTRL, whereas DAT remained unaffected by treatments ($F_{119} = 0.4$; $P = 0.62$). In particular, ANOVA calculated on both TH-positive ($F_{170} = 49.97$; $P < 0.0001$) and PSD-95–positive elements ($F_{128} = 36.89$; $P < 0.0001$) revealed statistical differences between experimental groups. Post hoc analysis showed a selective reduction of TH ($t = 7.42$; $P < 0.0001$) and PSD-95 ($t = 7.01$; $P < 0.0001$) density in EtOH-W vs. CTRL. Although the amount of TH and PSD-95 appears increased by 10% and 13%, respectively, it did not reach statistical significance in EtOH-CHR for either TH ($t = 1.39$; $P = 0.17$) or PSD-95 counts vs. CTRL (Fig. 4).

Patch-Clamp Analysis of GLUergic Excitatory Synapses in Nacc MSNs. Spontaneous miniature excitatory postsynaptic currents (mEPSCs) were recorded in voltage-clamped (−65 mV) MSNs of the Nacc shell in the presence of the γ-aminobutyric acid type A receptor antagonist bicuculline (20 μM) and the voltage-dependent Na^+ channel blocker lidocaine (500 μM) (Fig. 5 *A*–*C*). Recorded

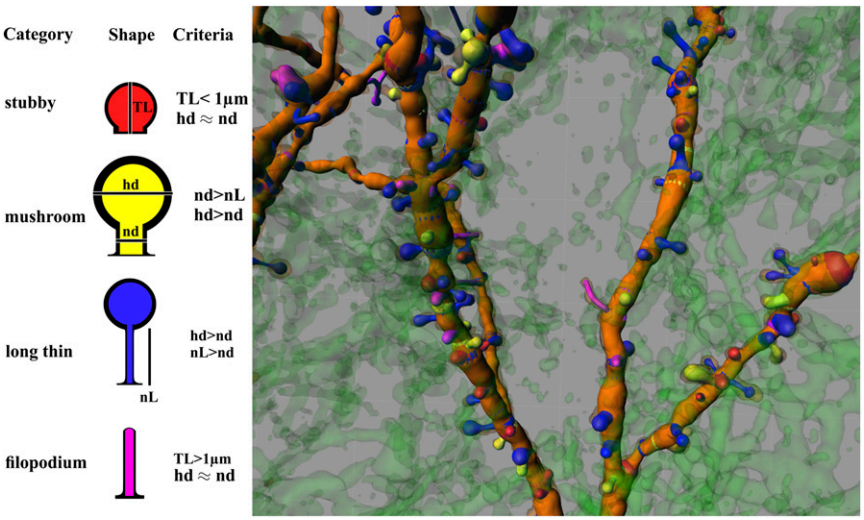

Fig. 1. Morphological and morphometrical characteristics used for spine classification. (*Left*) Four different morphological (shape) types were identified and categorized based on morphometrical features (criteria), as indicated. hd, head diameter; nd, neck diameter; nL, neck length; TL, total length. (*Right*) Example of a typical observation made on the dendritic tree of an MSN belonging to a rat of the control group. The image is color-coded. Colored bands on dendrites indicate the origin of spines.

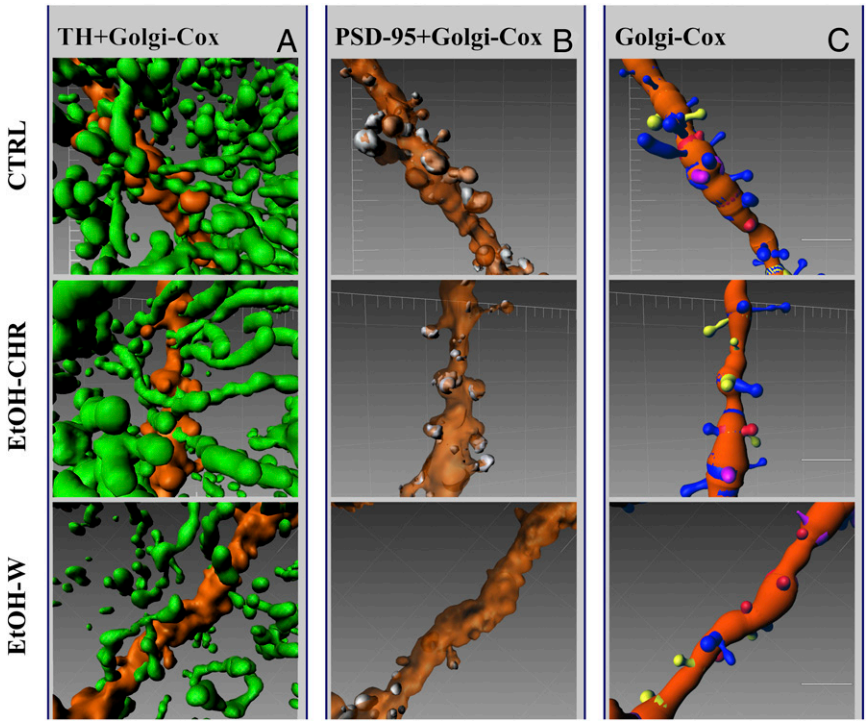

Fig. 2. Representative MSN dendritic branch (orange) showing anatomical differences among CTRL, EtOH-CHR, and EtOH-W groups in TH-positive fiber density (green) (*A*) and colocalized PSD-95 (white) (*B*). (*C*) Selective loss of long thin (blue) spines in the EtOH-W group. Colored bands on dendrites indicate the origin of spines. Software used was Imaris 7.4. (Scale bars, 5 μm.)

mEPSCs appear to be mediated by the α-amino-3-hydroxy-5-methyl-4-isoxazolepropionic acid (AMPA)/kainate type of GLU receptors, as they were completely suppressed by bath perfusion of the antagonist 6-cyano-7-nitroquinoxaline-2,3-dione (CNQX) (5 μM) (Fig. S4). One-way ANOVA of averaged mEPSCs revealed a significant effect of ethanol treatment on current amplitude ($F_{2,54} = 3.809$; $P < 0.05$), with a significant increase (20 ± 5.5%; $P < 0.05$) in EtOH-W rats compared with CTRL animals (Fig. 5 *B* and *C*). Ethanol withdrawal also altered mEPSC kinetics, with a significant ($P < 0.001$) increase in the slow but not fast component of the decay time relative to CTRL rats (Fig. 5 *B* and *D*); such an effect could be related to an increase in NR2C receptor subunit-mediated currents, as recently suggested (27) for core neurons. Furthermore, mEPSC frequency was markedly affected by ethanol treatment ($F_{2,52} = 12.52$; $P < 0.0001$), with a significant increase (68 ± 11%; $P < 0.0001$) found in EtOH-CHR and a reduction (27 ± 10%; $P < 0.05$) found in EtOH-W rats (Fig. 5 *A* and *E*). Likewise, a detailed analysis of mEPSC amplitude distribution revealed that chronic ethanol treatment and withdrawal affected mostly mEPSCs with lower amplitudes (Fig. S5).

Because changes in mEPSC frequency might be indicative of alterations in the presynaptic probability of GLU release, we next applied the paired-pulse (P-P) protocol, which consists of delivering two stimuli of the same intensity with an interevent interval of 50 ms, and the recording of the evoked AMPA receptor (r)-mediated EPSCs (Fig. 5 *F* and *G*). In MSNs from CTRL rats, the P-P ratio had a value of less than 1 (Fig. 5 *E* and *F*). Ethanol treatment produced a significant effect ($F_{2,18} = 16.01$; $P < 0.05$) on the P-P ratio, which was decreased in EtOH-CHR rats and increased in EtOH-W animals ($P < 0.05$), consistent with an enhancement and reduction of the probability of GLU release, respectively (Fig. 5 *E* and *F*).

We next recorded the evoked EPSCs (eEPSCs) mediated selectively by AMPA and *N*-methyl-D-aspartate (NMDA) receptors and calculated the NMDA:AMPA ratio (Fig. 6). EPSCs mediated by each receptor type were evoked by stimulation with increasing intensity (from 0.0 to 1.0 mA) to obtain an input–output (I–O) relationship. The I–O curve of AMPAr-medited EPSCs revealed that the value of stimulation intensity evoking a half-maximal response was not altered in ethanol-treated rats compared with CTRL, although in EtOH-W subjects there was a trend toward a decrease (13 ± 3.8%; $P = 0.052$) (Fig. 6 *A* and *B*). In contrast, in NMDAr-mediated EPSCs, ANOVA showed a significant effect of ethanol treatment between groups ($F_{2,21} = 5.229$; $P < 0.05$), with an increase (37 ± 6.6%; $P < 0.05$) of the value of the stimulation intensity evoking a half-maximal response in EtOH-W rats compared with CTRL animals (Fig. 6 *C* and *D*). Values of half-maximal current amplitude for each NMDAr and AMPAr (Fig. 6*E*) were used to calculate the NMDA:AMPA ratio, which was found significantly reduced (58 ± 19%; $P < 0.001$) in EtOH-W compared with CTRL rats (Fig. 6*F*).

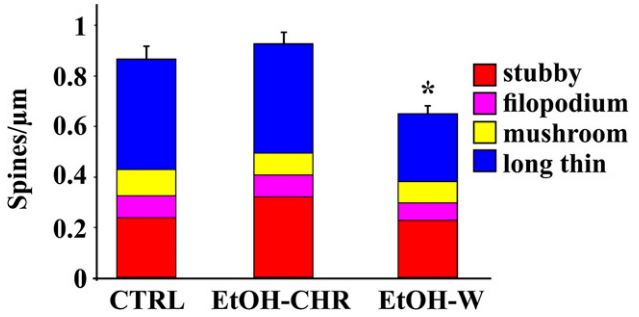

Fig. 3. Histograms represent the mean ± SEM of dendritic spine densities of second-order dendrites of NAcc shell MSNs in the three experimental conditions. Various spine typologies are represented within each group. *$P <$ 0.0001 vs. CTRL.

Long-Term Synaptic Plasticity of Excitatory GLUergic Synapses in Nacc MSNs. We next studied the effects of chronic ethanol treatment and withdrawal on the induction of LTD by measuring AMPAr-mediated EPSCs in single voltage-clamped MSNs of the Nacc shell as well as field excitatory postsynaptic potentials (fEPSPs) by extracellular recording in Nacc slices. In single voltage-clamped (−65 mV) MSNs of CTRL rats, low-frequency stimulation [LFS; 500 stimuli at 1 Hz, at a holding membrane potential (V_m) of −50 mV] induced a marked decrease (59 ± 3.3%) in EPSC amplitude when calculated during the final 20 min of recording relative to baseline (pre-LFS; 1) (Fig. 7 *A* and *B*). LTD formation appears to be dependent on the activation of NMDA receptors, as bath perfusion of (2*R*)-amino-5-phosphonopentanoate (APV) (50 μM) completely suppressed the long-term decrease in EPSC amplitude (Fig. S6). One-way ANOVA revealed a significant effect of ethanol treatment ($F_{2,17} = 10$; $P < 0.005$), with a reduction ($P < 0.005$) in EtOH-W compared with CTRL rats. LTD measured in EtOH-CHR was unaffected (Fig. 7 *A* and *B*).

Similar results were obtained when LTD was analyzed by extracellular recording of fEPSPs in slices containing the Nacc shell (Fig. 7*C*). LFS (500 stimuli at 1 Hz) produced a decrease in fEPSP slope that, when calculated during the last 20 min of recording, had values of 39 ± 3.3% and 29 ± 3.1% in CTRL and EtOH-CHR rats, respectively, compared with the slope of fEPSPs at baseline (Fig. 7 *C* and *D*). In EtOH-W rats, LFS resulted in a decrease in fEPSP slope of only 5 ± 1.4% (vs. baseline), and this effect was statistically significant compared with CTRL animals ($F_{2,17} = 10$; $P < 0.05$).

Effects of Chronic Ethanol Treatment and Withdrawal on Passive Membrane Properties and Excitability of Nacc Shell MSNs. Consistent with previous reports (28), MSNs of Nacc are typically hyperpolarized, with a mean resting V_m of −77 ± 1.2 mV ($n = 28$) in CTRL, −69 ± 1.8 ($n = 20$) in EtOH-CHR, and −81 ± 0.8 mV ($n = 9$) in EtOH-W rats. Membrane capacitance of MSNs was measured and one-way ANOVA revealed an effect of EtOH treatment ($F_{2,74} = 3.84$; $P < 0.05$), with a significant reduction (17 ± 3.9%; $P < 0.05$) in EtOH-W but not in EtOH-CHR (Fig. 8*A*). Further, we found a significant effect on the slope of the voltage/current intensity (V/I) curve (Fig. 8*C*), consistent with an increase (33 ± 5.7%) of input resistance (R_{in}) in EtOH-W rats compared with CTRL animals ($F_{2,57} = 3.961$; $P < 0.05$) (Fig. 8*D*). Injection of depolarizing currents (20–300 pA) resulted in a depolarization-dependent increase of the action potential (AP) firing rate (Fig. 8 *E–I*). We observed no significant difference in AP threshold between the two groups of EtOH-treated and CTRL rats (Fig. 8*F*). However, the value of the minimum current step, needed to evoke the first AP, was significantly decreased (Fig. 8*G*) in both EtOH-CHR and EtOH-W rats compared with CTRL animals ($F_{2,57} = 3.607$; $P < 0.05$). In addition, evaluation of AP latency revealed a significant difference between groups ($F_{2,1140} = 32.90$; $P < 0.0001$). Post hoc analysis showed that in EtOH-CHR and EtOH-W, AP latency was significantly decreased ($P < 0.001$) compared with CTRL animals (Fig. 8 *E* and *H*). Furthermore, ANOVA also revealed a significant change in the effect of the depolarization step-dependent increase of the AP firing rate between groups ($F_{2,1140} = 16.34$; $P < 0.0001$), with a significant increase in EtOH-treated rats ($P < 0.0001$; Fig. 8 *E* and *I*).

Discussion

Ethanol withdrawal signs and symptoms emerge when prolonged ethanol consumption is abruptly discontinued. Thus, ethanol withdrawal is experimentally appealing for studying the effects of chronic ethanol intake and its sudden suspension.

In this study, rats were subjected to a 20-d continuous ethanol exposure through a liquid diet, and the results show that such treatment determines a state of dependence; in fact, suspension of ethanol availability induced a typical withdrawal syndrome, as indexed by somatic withdrawal signs. In these ethanol-dependent animals, our main objective was to carefully examine, by using a multiple approach involving morphological/immunohistochemical and functional analysis, the effects of chronic ethanol exposure and subsequent withdrawal on GLUergic and DAergic signaling in medium spiny neurons of the Nacc shell.

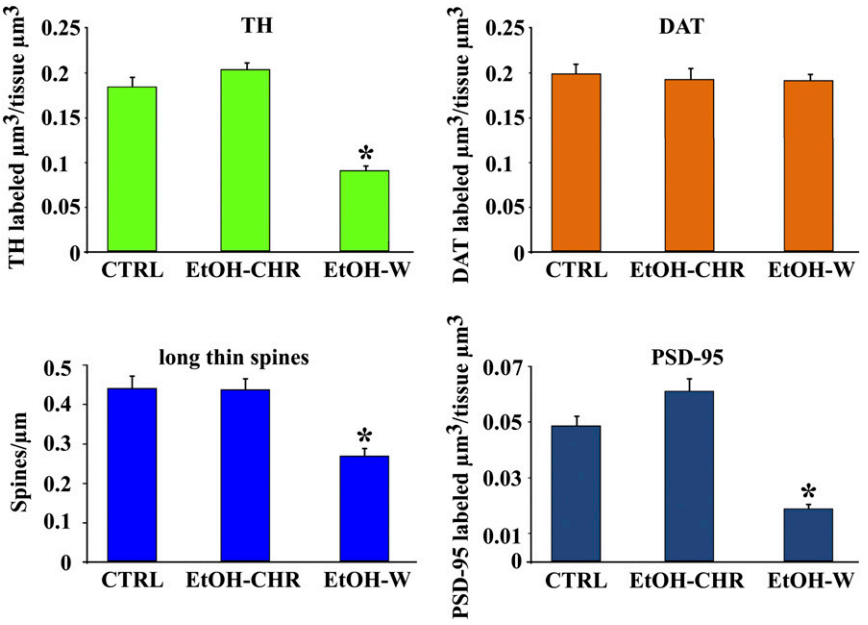

Fig. 4. Depiction of changes affecting presynaptic (*Upper*) and postsynaptic indices (*Lower*) observed in the three experimental conditions. (*Upper*) TH volume (*Left*) is halved by EtOH-W and unaltered by EtOH-CHR, whereas DAT (*Right*) is unmodified by treatments. (*Lower*) Long thin spine density (*Left*) is reduced by about 40%, and this effect is paralleled by a reduction in PSD-95 (*Right*) immunolabeling of similar proportions (~60%). *$P < 0.0001$ vs. CTRL. Error bars represent SEM in all figures.

One of the main findings of the present work rests on the simultaneous visualization of dendritic spines and immunoreactivity of TH, DAT, and PSD-95. Indeed, we were able to distinguish the various subtypes of spines with Golgi-Cox staining and attribute immunoreactivity to each of them. We observed a marked reduction of TH-positive fibers, whereas DAT immunoreactivity was unaffected by EtOH treatments. Thus, TH-containing terminals appear to be present unmodified, but TH quantity, and presumably DA synthesis, is reduced in EtOH-W. Although we did not measure other indices of DA signaling in the present work, such changes are consistent with previous reports (20), and further add to the idea of a reduction in DAergic firing and DA microdialysates observed in the Nacc of rats suspended from chronic ethanol administration (29). In addition, PSD-95 immunoreactivity and spine density are similarly reduced in ethanol-withdrawn rats, compared with animals that were tested while still intoxicated, thereby suggesting, as a whole, yet another example of aberrant structural synaptic plasticity that takes place in association with ethanol withdrawal, a crucial phase of ethanol dependence. Further, the results also suggest a correlation between ethanol-induced modifications of DAergic transmission and remodeling of dendritic spines. Thus, we hypothesize here a close relationship between the ethanol withdrawal-induced reduction of DAergic activity and the loss of dendritic spines in the Nacc shell. Such a conclusion would also be consistent with results obtained using 6-hydroxydopamine lesions (30) and the consequent marked decrease in MSN spine density (31–33). It is also supported by previous data showing that morphine-withdrawn (34) and cannabis-dependent subjects (35) display a loss of dendritic spines paralleled by a reduced DAergic firing (36, 37) and impaired DA release (38–40). Alternatively, and/or in addition to the previous interpretation, evidence for occlusion of LTD in ethanol-withdrawn rats can stem from the decreased spine density, shrinkage, and synaptic loss in this group of animals. On the other hand, the decrease in NMDAr-mediated synaptic responses (see below) might cause a shift in the threshold for LTD induction in ethanol withdrawal. Quantitatively, total spine density is reduced 25% by EtOH-W, but the reduction approximates 40% if compared with long thin spines (which is the only spine typology affected). This is reminiscent of the decrement observed for DAergic (TH) and GLUergic (PSD-95) signaling, thereby strengthening the view of a link between pre- (DA) and post- (spine PSD-95) synaptic indices in EtOH-W.

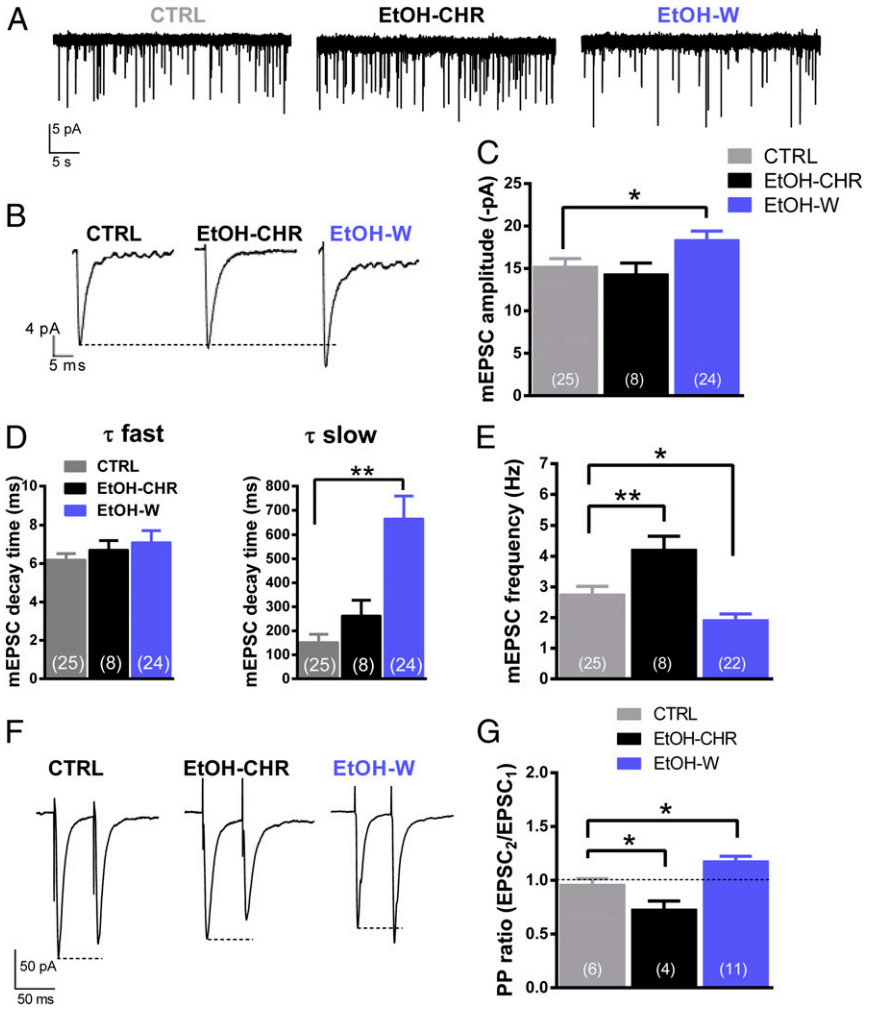

Fig. 5. Effects of chronic ethanol treatment and withdrawal on GLUergic mEPSCs and paired-pulse ratio measured in MSNs of the Nacc. (*A*) Representative tracings of mEPSCs from single voltage-clamped MSNs of the different experimental groups. (*B*) Averaged mEPSCs recorded during periods of 3 min from which analysis of the kinetic properties has been conducted. (*C–E*) The bar graphs summarize changes in mEPSC amplitude, fast and slow decay time constants, and frequency, and are expressed as the mean of absolute values ± SEM. (*F*) Representative traces of averaged synaptically evoked EPSCs obtained with an interstimulus of 50 ms. (*G*) Paired-pulse ratio in the different experimental groups. The number of cells analyzed is indicated in each bar. $*P < 0.05$, $**P < 0.001$ vs. CTRL.

The selective loss of thin spines as a consequence of ethanol withdrawal, observed in the present study, is consistent with a model in which the spine volume and spine density changes regulate the anatomy and activity of the network between prosencephalic and mesencephalic areas. Indeed, whereas long-term potentiation (LTP) requires spine head enlargement (41), with recruitment of additional AMPA-type glutamate receptors (42, 43), LTD is associated with spine loss (44), which, in turn, may be dependent upon actin turnover (44), thereby altering regulation of the actin cytoskeleton structure (45).

Our functional analysis has indeed provided evidence that, in association with changes in dendritic spine density and synaptic protein expression, ethanol withdrawal produces profound alterations in both GLUergic synaptic transmission and plasticity. Accordingly, we found that ethanol withdrawal dramatically decreased the formation of LTD, as indexed by both patch-clamp and extracellular recordings of EPSCs and fEPSPs, respectively. On the other hand, LTD formation was unmodified in chronically ethanol-treated rats killed while still intoxicated, an observation that strengthens the correlation between morphological and functional changes occurring during ethanol withdrawal. As previously reported (46, 47), in single Nacc MSNs, low-frequency stimulation (500 stimuli at 1 Hz) paired with postsynaptic membrane depolarization (−50 mV) resulted in the induction of LTD, which is dependent on the activation of NMDA receptors, as it is completely prevented by the NMDAr antagonist APV. Jeanes and colleagues (47) additionally demonstrated that in Nacc MSNs, LTD could require NMDA receptors that selectively contain the NR2B subunit, which is highly expressed in these neurons (48), as LTD formation could be prevented by the application of the selective antagonist Ro 25-6981. Blockade of NMDAr-dependent LTD in Nacc MSNs was detected in mice that were exposed to a single bout of chronic intermittent ethanol and tested 24 h after withdrawal (47). Interestingly, such exposure produced metaplasticity with a conversion of LTD to an NMDAr-dependent LTP and, after 3 d of withdrawal, both LTD and LTP were undetected. In our study we did not observe such metaplasticity, but the marked difference in the ethanol-treatment protocols (continuous versus intermittent exposure) used may certainly contribute to explaining such diversity. Blockade of NMDAr-dependent LTD following ethanol withdrawal was also reported in the hippocampal CA1 region of rats that had been exposed to a liquid diet containing ethanol for 38–41 wk (49). Thus, impairment of NMDAr-dependent LTD appears to represent a consistent effect that takes place at excitatory synapses of different brain regions as a consequence of ethanol withdrawal.

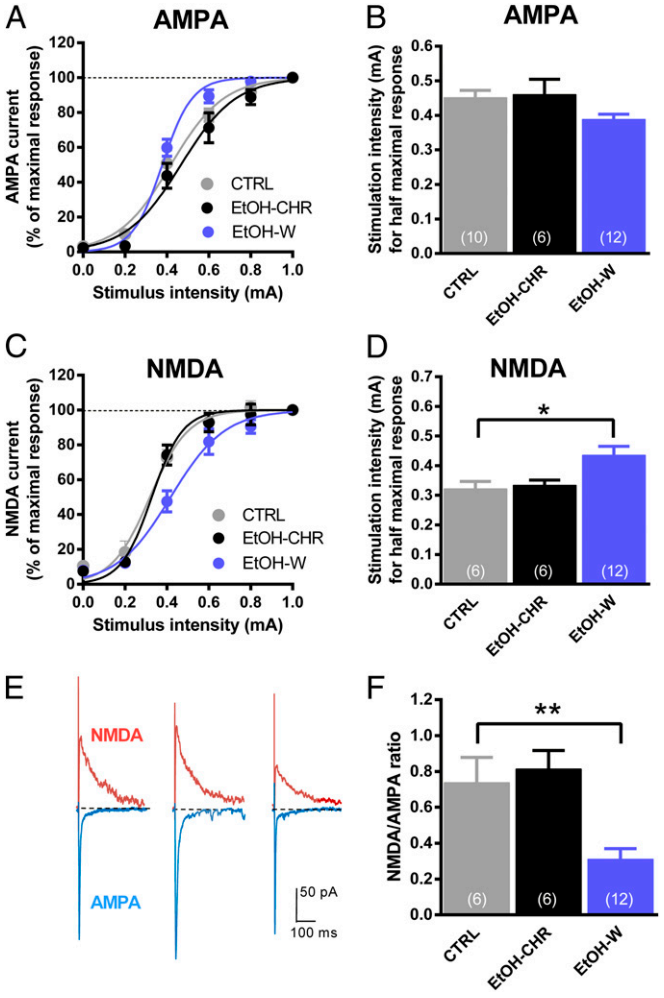

Fig. 6. Changes in NMDA:AMPA ratio in Nacc MSNs induced by chronic ethanol exposure and withdrawal. I–O curves of AMPAr- (*A*) and NMDAr-mediated (*C*) eEPSCs. The values represent current amplitude and are normalized to the maximal response. (*B* and *D*) The graphs summarize the values of stimulus intensity that evoked a half-maximal response in the different experimental groups. Data are expressed as averaged absolute values ± SEM. (*E*) Representative eEPSCs mediated by NMDA and AMPA receptors recorded in single MSNs. (*F*) The graph summarizes the NMDA:AMPA ratio obtained from MSNs of the different experimental groups. The number of cells analyzed is indicated in each bar. $*P < 0.05$, $**P < 0.001$ vs. CTRL.

Recordings of NMDAr- and AMPAr-mediated EPSCs in voltage-clamped Nacc MSNs provide further hints on the possible neurochemical and functional alterations that may be crucial in contributing to the reduction of LTD in ethanol-withdrawn rats. In fact, calculation of the NMDA:AMPA ratio revealed that this postsynaptic parameter was significantly reduced in EtOH-W rats compared with EtOH-CHR. Such an effect appears to result, in part, from the marked reduction in NMDAr function, as indicated by the right shift of the corresponding I–O relationship (Fig. 6). Thus, a reduced NMDAr function associated with ethanol withdrawal is consistent with the decreased immunoreactivity for PSD-95 that plays a crucial role as an anchoring protein for NMDA receptors in the spine membrane (50). Altogether, these data led us to hypothesize that in Nacc shell MSNs, ethanol withdrawal-induced DAergic blunting, through the reduced expression of PSD-95 and associated long thin spine loss, impairs NMDAr signaling, an effect that in turn may lead to dampening of LTD formation in these synapses. Similarly, in the hippocampus, spine loss and shrinkage have been causally linked to LTD (51, 52).

In addition, ethanol withdrawal was also associated with an increase in AMPAr-mediated excitatory transmission, as indexed by enhancement of mEPSC amplitude together with a slight shift of the I–O curve. This finding appears to be consistent with data obtained recently in MSNs of the primate putamen (53) and rat Nacc core following chronic intermittent ethanol exposure and withdrawal (54). In the latter study, the increased AMPAr-mediated mEPSC amplitude was associated with enhanced membrane insertion of GluA-lacking AMPA receptors, which are characterized by high unitary channel conductance (55). Consistent with previous studies in rodents and nonhuman primates (53, 54), ethanol withdrawal was accompanied by an increased MSN intrinsic excitability. Such an effect was not associated with altered AP threshold value, but could possibly be related to the increased input resistance that predicts a higher voltage change (i.e., higher depolarization) in response to a cationic current.

DA neurons originating in the VTA, and innervating MSNs, represent a major substrate involved at molecular (56), cellular (9, 57), and behavioral levels (58, 59). In particular, it has

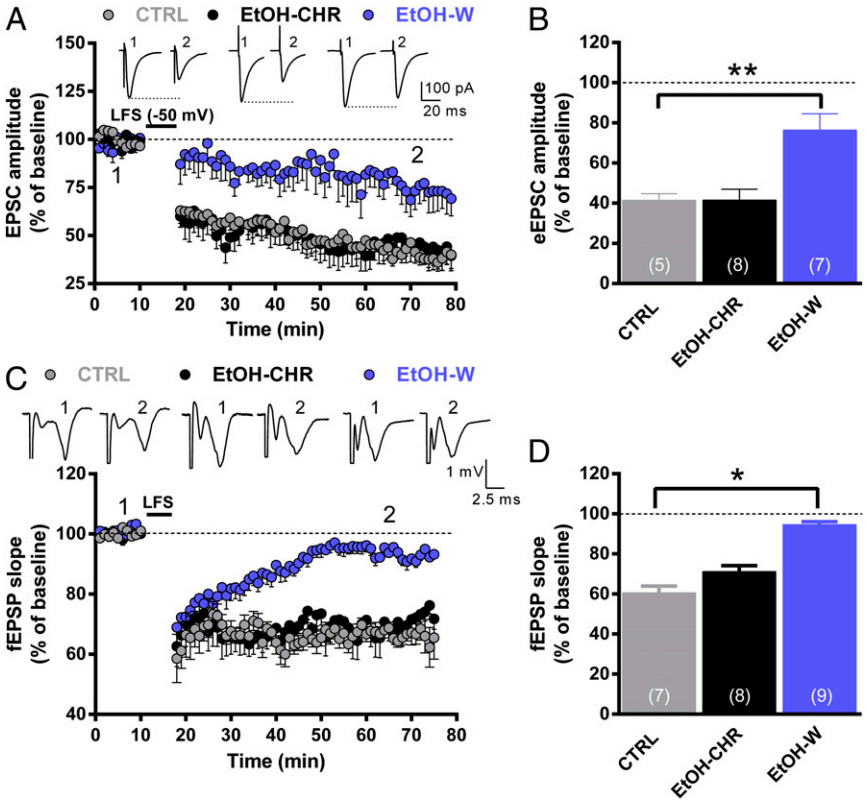

Fig. 7. Effect of chronic ethanol treatment and withdrawal on LTD induced in Nacc MSNs. (*A*) AMPAr-mediated EPSCs were recorded in single voltage-clamped (−65 mV) MSNs of the Nacc shell obtained from the different groups of animals. Representative EPSCs recorded before (1) and after (2) conditioning are shown above the graph. (*B*) The graph illustrates the degree of LTD, calculated by averaging the percent change in EPSC amplitude from baseline 70–80 min after LFS. The number of cells analyzed is indicated in each bar. $^{**}P < 0.01$ vs. CTRL. (*C*) Field EPSPs were recorded in Nacc shell slices obtained from the different groups of rats. LTD was elicited by LFS (500 stimuli at 1 Hz), and representative traces are shown above the graph. Data are expressed as mean percent change in fEPSP slope ± SEM from baseline. (*D*) The graph summarizes the degree of LTD, calculated by averaging the percentage change in fEPSP slope from baseline 70–80 min after LFS. The number of recordings analyzed is indicated in each bar. $^{*}P < 0.05$ vs. CTRL.

been hypothesized that withdrawal after chronic administration of numerous drugs of abuse produces a hypodopaminergic state (2, 12). Consistently, the observed reduction in TH immunoreactivity in the Nacc shell during ethanol withdrawal can be related to (and parallels) deficiencies in DA release (60) and decrements in neuronal activity observed in similar contexts (29, 61). If so, the primary cause of the dendritic remodeling and spine pruning reported in our study could be due to the impairment in DA signaling (29, 60), consequent to ethanol abrupt abstinence. This double DAergic and GLUergic dysfunction may yield increased intraspinous calcium levels, which foster changes in spine morphology and fast shrinkage and collapse of spines, thereby preventing LTD formation, eventually (62).

As a whole, these architectural modifications in synaptic connections in the Nacc, involving three major players of intra- (and extra-) Nacc physiology, may underlie the aberrant behavior of alcohol abuse/dependence, and restoring DAergic and/or GLUergic functioning may contribute to restoring spine physiological integrative properties (63). Elucidating this role could have implications for understanding the physiopathology of alcoholism.

Materials and Methods

The study was carried out in accordance with the current Italian legislation (D.L. 116, 1992), which allows experimentation on laboratory animals only after submission and approval of a research project to the Committee of Bioethics for Animal Testing (Sassari, Italy) and to the Ministry of Health (Rome), and in strict accordance with the European Council directives on the matter (2007/526/CE). All possible efforts were made to minimize animal pain and discomfort and to reduce the number of experimental subjects.

Animals. Male Wistar rats (Harlan) ($n = 25$), weighing 125–155 g at the beginning of treatment, were housed individually in Plexiglas cages and fed a liquid diet, continuously available, containing 910–970 mL fresh whole cow's milk (CoaPla), 5,000 IU/L vitamin A, and 17 g/L sucrose. This mixture supplies 1000.7 kcal/L, according to the method of Uzbay and colleagues (64). No extra chow or water was supplied. The colony room was maintained under controlled environmental conditions (temperature, 22 ± 2 °C; humidity, 60–65%) on a reverse 12-h light/dark cycle. All behavioral experimental sessions were conducted during the dark phase and were carried out in the same colony room.

Ethanol Dependence Induction. The diet (64) was gradually enriched with 2.4% (days 1–4), 4.8% (days 5–8), and 7.2% (days 9–20) ethanol and administered for 20 d. The weight, as well as liquid intake, of the rats was monitored daily. Ethanol intake was measured and expressed as g/kg. Blood ethanol levels were measured as follows: blood samples (50 μL) were collected from the tip of the tail of each rat. Blood samples were analyzed by means of an enzymatic system (GL5 Analyzer; Analox Instruments) based on measurement of oxygen consumption in the alcohol-acetaldehyde reaction. Control rats were pair-fed with a liquid diet (no ethanol).

Upon suspension of the ethanol-enriched diet, rats were divided into two subgroups: EtOH-CHR (within 30 min of liquid diet removal) and EtOH-W (12 h from ethanol suspension), and withdrawal signs were scored by an experimenter blind to the treatments. Withdrawal signs—body tremors, tail rigidity, irritability to touch (vocalization), and ventromedial limb retraction—were observed for 5 min in an observation chamber. To measure anxiety-like responses, the elevated plus maze test was used. The apparatus consisted of two gray Plexiglas open arms and two black enclosed arms (40-cm high walls), arranged such that the respective arms were opposite each other. The 5-min test procedure began when the animal was placed in the center of the maze, facing an open arm. The percentage of time spent in the open arms and the percentage of open-arm entries were scored and used as a measure of anx-

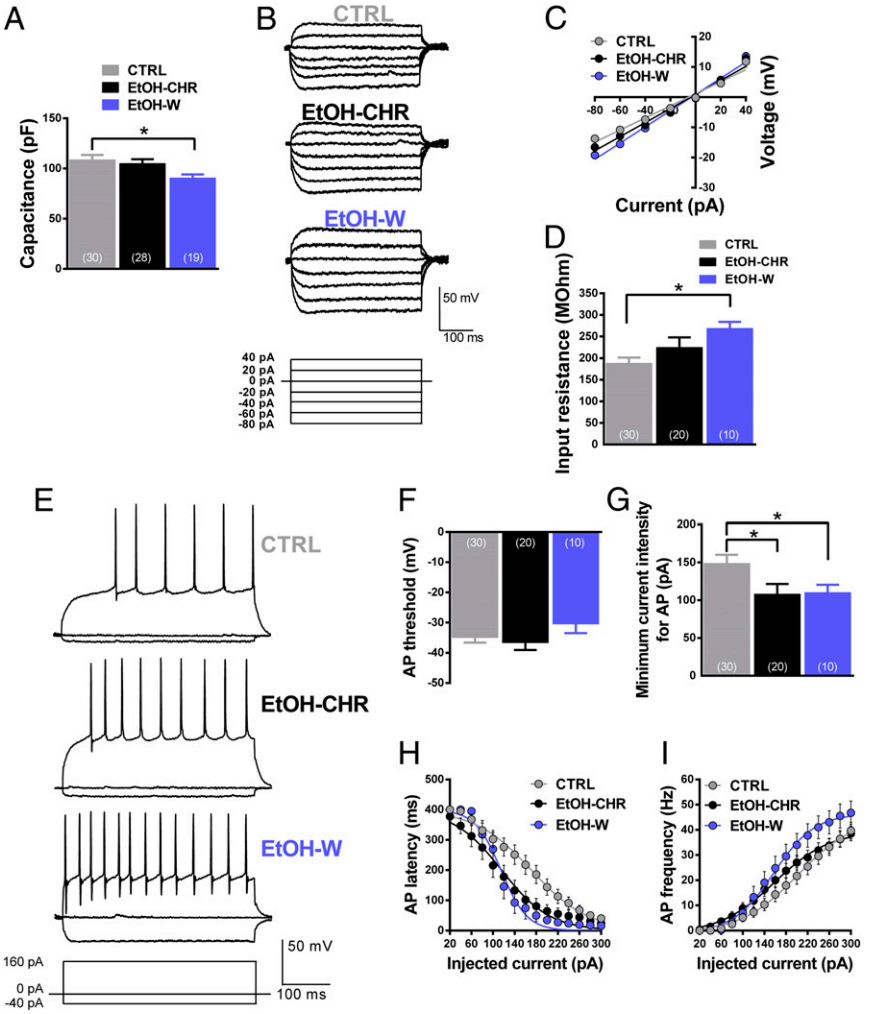

Fig. 8. Effects of chronic ethanol treatment and withdrawal on passive membrane properties and excitability of Nacc MSNs. (*A*) The graph summarizes changes in membrane capacitance observed in different experimental groups. Data are expressed as absolute values (pF) and are means ± SEM from the number of cells indicated in each bar. *$P < 0.05$ vs. CTRL. (*B*) Representative voltage responses to negative and subthreshold positive current pulses applied to MSNs in current-clamp mode. (*C* and *D*) V/I relationship (*C*) and comparison of membrane input resistance (*D*) (MΩ). *$P < 0.05$ vs. CTRL. (*E*) Representative membrane voltage responses to negative (−20 pA) and positive (160 pA) pulses. (*F–I*) Effects of chronic ethanol treatment and withdrawal on action potential threshold (*F*), minimum current intensity required for inducing the first AP (*G*), AP latency (*H*), and AP frequency (*I*). Data are expressed as means ± SEM from the number of cells indicated in each bar. *$P < 0.05$ vs. CTRL.

iety-like behavior across groups. Withdrawal signs were scored using a rating scale adapted from Macey and colleagues (65) as follows: 0, no sign; 1, moderate; 2, severe.

Histology. ***Golgi-Cox staining and immunofluorescence.*** Rats were deeply anesthetized with chloral hydrate and perfused intracardially with 0.9% saline solution followed by 4% (vol/vol) paraformaldehyde. Brains were carefully removed from the skull and processed as already described in detail (23) (Movie S1). Briefly, after the Golgi-Cox procedure, 50-μm coronal slices were cut, developed, and collected in phosphate buffer for free-floating immunostaining. Slices were preincubated in 5% normal goat serum, 5% BSA, 5% normal donkey serum, and 1% Triton X-100 in PBS overnight at 4 °C. Three primary antibodies were used: polyclonal rabbit anti-TH (1:200), monoclonal mouse anti–PSD-95 (1:200) (Santa Cruz Biotechnology), and rat monoclonal anti-DAT (1:200) (Millipore) for 48 h at 4 °C. Slices were then incubated in a mixture of fluorescein/streptavidin (Vector Laboratories) (1:200) and anti-rabbit Alexa Fluor 546 (1:200) (Molecular Probes), biotinylated goat anti-rat IgG (Vector Laboratories), and Alexa Fluor 488-conjugated streptavidin (Jackson ImmunoResearch) secondary antibodies for 3 h at room temperature.

Laser Scanning Confocal Microscopy. Analysis was performed using a Leica 4D confocal laser scanning microscope with an argon/krypton laser. Confocal images (512 × 512 pixels; pixel size: 0.2 μm X; 0.2 μm Y; 0.5 μm Z) were generated using PL Fluotar 40× oil (n.a. 1.00) and 100× oil (n.a. 1.3). Pinhole: 0.5 airy units.

TH, DAT, PSD-95, and Spine Counts. For counts, confocal images (Fig. S3*A*) were obtained 24 h after the immunofluorescence procedure. TH, DAT, and PSD-95 volumes were determined as follows: each dataset (70–80 images) was composed for each of the three channels (fluorescein, rhodamine, and reflection) using identical laser and microscope settings. Four regions of interest (*x*, 40 μm; *y*, 40 μm; *z*, 10 μm) were randomly chosen and, in each one, virtual objects (Fig. S3*B*) were created and their volume was calculated, summed, and expressed as volume per μm^3 ($n = 120$). Threshold, defined as the gray value below which signal is considered background, was set at 70–90 for Golgi-Cox, 30–40 for PSD-95, and 50–60 for TH and DAT on a scale of 0 to 255 of gray values.

For spine density evaluation, $n = 120$ dendritic segments (at least 20 μm long) from shell MSN were collected and both manually (Bioscan Optimas 6.5.1) and automatically (filament tool; Bitplane Imaris 7.4) counted. Primary dendrites innervated primarily by inputs of intrinsic origin (66) were not considered.

Electrophysiology. Coronal brain slices containing the NAcc shell region were prepared as previously described for hippocampus (67). For all recordings performed in MSNs of the Nacc shell, the temperature of the bath was

maintained at 33 °C. For patch-clamp recordings, GLUergic excitatory postsynaptic currents (mEPSCs, eEPSCs) were recorded with an Axopatch 200B amplifier, filtered at 2 kHz, and digitized at 5 kHz. AMPAr-mediated eEPSCs were recorded at a holding potential of −65 mV, whereas NMDAr-mediated responses were recorded at a holding potential of 40 mV in the presence of the AMPA/kainate receptor antagonist CNQX (5 mM). Access resistance ranged from 15 to 30 MΩ and was monitored throughout the recording by injection of 10-mV hyperpolarizing pulses. If it changed during recording more than 20%, the cell was discarded from analysis. Analysis of mEPSCs was performed manually using Mini analysis software (Synaptosoft, Inc., version 6.0.2) with a noise amplitude threshold of 2 pA. Best decay fit calculation was made by a two-parameter peak-to-end detection. For LTD experiments, eEPSCs were recorded in voltage-clamped (−65 mV) MSNs at a frequency of 0.05 Hz (baseline); an LFS (500 stimuli at 1 Hz) paired with membrane depolarization (holding potential; −50 mV) was then applied, and eEPSCs were then recorded for the following 60 min at 0.05 Hz. The paired-pulse protocol consisted of delivering two consecutive electrical stimuli with an interevent interval of 50 ms, and the ratio of the amplitude of the second eEPSC and that of the first was calculated. For fEPSPs, responses were triggered digitally every 20 s by application of a constant current pulse of 0.2–0.4 mA with a duration of 60 μs, which yielded a half-maximal response. The fEPSPs were amplified with the use of an Axoclamp 2B amplifier (Axon Instruments), digitized, and then analyzed with Clampfit 9.02 software (Axon Instruments). For induction of LTD, after 10 min of stable baseline recording of fEPSPs evoked every 20 s at the current intensity that triggered 50% of the maximal fEPSP response, LFS (500 stimuli at 1 Hz) was applied. In addition, passive membrane properties (R_{in}, capacitance) as well as intrinsic excitability were evaluated.

Statistical Analysis. Analysis of variance (one- or two-way ANOVA) followed by Tukey, least significant difference, or Student *t* post hoc test was used. Withdrawal signs were assessed by individual comparison among individual means using the nonparametric Mann–Whitney *U* test. All values are expressed as mean (±SEM) unless otherwise indicated. A P value of <0.05 was considered statistically significant for all experiments.

ACKNOWLEDGMENTS. The authors thank A. T. Peana for assisting in anxiety evaluation, G. Colombo for helpful discussions, and M. C. Mostallino and P. P. Secci at Sardegna Ricerche for assistance in using the confocal microscope and other facilities. This work was supported in part by funds from Regione Autonoma della Sardegna, Progetti di Ricerca di Base, Bando 2008 (to M.D.) and Bando 2010 (to E.S.).

1. Bouchery EE, Harwood HJ, Sacks JJ, Simon CJ, Brewer RD (2011) Economic costs of excessive alcohol consumption in the U.S., 2006. *Am J Prev Med* 41(5):516–524.
2. Melis M, Spiga S, Diana M (2005) The dopamine hypothesis of drug addiction: Hypodopaminergic state. *Int Rev Neurobiol* 63:101–154.
3. Kalivas PW, Brady K (2012) Getting to the core of addiction: Hatching the addiction egg. *Nat Med* 18(4):502–503.
4. Koob GF, Volkow ND (2010) Neurocircuitry of addiction. *Neuropsychopharmacology* 35(1):217–238.
5. Edwards S, Koob GF (2010) Neurobiology of dysregulated motivational systems in drug addiction. *Future Neurol* 5(3):393–401.
6. Floresco SB, Todd CL, Grace AA (2001) Glutamatergic afferents from the hippocampus to the nucleus accumbens regulate activity of ventral tegmental area dopamine neurons. *J Neurosci* 21(13):4915–4922.
7. Nicola SM, Surmeier J, Malenka RC (2000) Dopaminergic modulation of neuronal excitability in the striatum and nucleus accumbens. *Annu Rev Neurosci* 23:185–215.
8. Floresco SB, Blaha CD, Yang CR, Phillips AG (2001) Modulation of hippocampal and amygdalar-evoked activity of nucleus accumbens neurons by dopamine: Cellular mechanisms of input selection. *J Neurosci* 21(8):2851–2860.
9. Pulvirenti L, Diana M (2001) Drug dependence as a disorder of neural plasticity: Focus on dopamine and glutamate. *Rev Neurosci* 12(2):141–158.
10. Javitt DC, et al. (2011) Translating glutamate: From pathophysiology to treatment. *Sci Transl Med* 3(102):102mr2.
11. Reissner KJ, Kalivas PW (2010) Using glutamate homeostasis as a target for treating addictive disorders. *Behav Pharmacol* 21(5-6):514–522.
12. Diana M (2011) The dopamine hypothesis of drug addiction and its potential therapeutic value. *Front Psychiatry* 2:64.
13. Freund TF, Powell JF, Smith AD (1984) Tyrosine hydroxylase-immunoreactive boutons in synaptic contact with identified striatonigral neurons, with particular reference to dendritic spines. *Neuroscience* 13(4):1189–1215.
14. Carr DB, Sesack SR (1996) Hippocampal afferents to the rat prefrontal cortex: Synaptic targets and relation to dopamine terminals. *J Comp Neurol* 369(1):1–15.
15. Sulzer D, et al. (1998) Dopamine neurons make glutamatergic synapses in vitro. *J Neurosci* 18(12):4588–4602.
16. Bérubé-Carrière N, et al. (2009) The dual dopamine-glutamate phenotype of growing mesencephalic neurons regresses in mature rat brain. *J Comp Neurol* 517(6):873–891.
17. Koos T, Tecuapetla F, Tepper JM (2011) Glutamatergic signaling by midbrain dopaminergic neurons: Recent insights from optogenetic, molecular and behavioral studies. *Curr Opin Neurobiol* 21(3):393–401.
18. Diana M, et al. (2003) Enduring effects of chronic ethanol in the CNS: Basis for alcoholism. *Alcohol Clin Exp Res* 27(2):354–361.
19. Kroener S, et al. (2012) Chronic alcohol exposure alters behavioral and synaptic plasticity of the rodent prefrontal cortex. *PLoS ONE* 7(5):e37541.
20. Rothblat DS, Rubin E, Schneider JS (2001) Effects of chronic alcohol ingestion on the mesostriatal dopamine system in the rat. *Neurosci Lett* 300(2):63–66.
21. Ortiz J, et al. (1995) Biochemical actions of chronic ethanol exposure in the mesolimbic dopamine system. *Synapse* 21(4):289–298.
22. Lee KW, et al. (2006) Cocaine-induced dendritic spine formation in D1 and D2 dopamine receptor-containing medium spiny neurons in nucleus accumbens. *Proc Natl Acad Sci USA* 103(9):3399–3404.
23. Spiga S, et al. (2011) Simultaneous Golgi-Cox and immunofluorescence using confocal microscopy. *Brain Struct Funct* 216(3):171–182.
24. Kasai H, et al. (2010) Learning rules and persistence of dendritic spines. *Eur J Neurosci* 32(2):241–249.
25. Lendvai B, Stern EA, Chen B, Svoboda K (2000) Experience-dependent plasticity of dendritic spines in the developing rat barrel cortex in vivo. *Nature* 404(6780):876–881.
26. Trachtenberg JT, et al. (2002) Long-term in vivo imaging of experience-dependent synaptic plasticity in adult cortex. *Nature* 420(6917):788–794.
27. Seif T, et al. (2013) Cortical activation of accumbens hyperpolarization-active NMDARs mediates aversion-resistant alcohol intake. *Nat Neurosci* 16(8):1094–1100.
28. O'Donnell P, Grace AA (1993) Physiological and morphological properties of accumbens core and shell neurons recorded in vitro. *Synapse* 13(2):135–160.
29. Diana M, Pistis M, Carboni S, Gessa GL, Rossetti ZL (1993) Profound decrement of mesolimbic dopaminergic neuronal activity during ethanol withdrawal syndrome in rats: Electrophysiological and biochemical evidence. *Proc Natl Acad Sci USA* 90(17):7966–7969.
30. Ingham CA, Hood SH, Arbuthnott GW (1989) Spine density on neostriatal neurones changes with 6-hydroxydopamine lesions and with age. *Brain Res* 503(2):334–338.
31. McNeill TH, Brown SA, Rafols JA, Shoulson I (1988) Atrophy of medium spiny I striatal dendrites in advanced Parkinson's disease. *Brain Res* 455(1):148–152.
32. Arbuthnott GW, Ingham CA, Wickens JR (2000) Dopamine and synaptic plasticity in the neostriatum. *J Anat* 196(Pt 4):587–596.
33. Villalba RM, Lee H, Smith Y (2009) Dopaminergic denervation and spine loss in the striatum of MPTP-treated monkeys. *Exp Neurol* 215(2):220–227.
34. Spiga S, Puddu MC, Pisano M, Diana M (2005) Morphine withdrawal-induced morphological changes in the nucleus accumbens. *Eur J Neurosci* 22(9):2332–2340.
35. Spiga S, Lintas A, Migliore M, Diana M (2010) Altered architecture and functional consequences of the mesolimbic dopamine system in cannabis dependence. *Addict Biol* 15(3):266–276.
36. Diana M, Pistis M, Muntoni A, Gessa G (1995) Profound decrease of mesolimbic dopaminergic neuronal activity in morphine withdrawn rats. *J Pharmacol Exp Ther* 272(2):781–785.
37. Diana M, Melis M, Muntoni AL, Gessa GL (1998) Mesolimbic dopaminergic decline after cannabinoid withdrawal. *Proc Natl Acad Sci USA* 95(17):10269–10273.
38. Pothos E, Rada P, Mark GP, Hoebel BG (1991) Dopamine microdialysis in the nucleus accumbens during acute and chronic morphine, naloxone-precipitated withdrawal and clonidine treatment. *Brain Res* 566(1-2):348–350.
39. Rossetti ZL, Hmaidan Y, Gessa GL (1992) Marked inhibition of mesolimbic dopamine release: A common feature of ethanol, morphine, cocaine and amphetamine abstinence in rats. *Eur J Pharmacol* 221(2-3):227–234.
40. Tanda G, Loddo P, Di Chiara G (1999) Dependence of mesolimbic dopamine transmission on delta9-tetrahydrocannabinol. *Eur J Pharmacol* 376(1-2):23–26.
41. Matsuzaki M, Honkura N, Ellis-Davies GC, Kasai H (2004) Structural basis of long-term potentiation in single dendritic spines. *Nature* 429(6993):761–766.
42. Nusser Z, et al. (1998) Cell type and pathway dependence of synaptic AMPA receptor number and variability in the hippocampus. *Neuron* 21(3):545–559.
43. Kharazia VN, Weinberg RJ (1999) Immunogold localization of AMPA and NMDA receptors in somatic sensory cortex of albino rat. *J Comp Neurol* 412(2):292–302.
44. Okamoto K, Nagai T, Miyawaki A, Hayashi Y (2004) Rapid and persistent modulation of actin dynamics regulates postsynaptic reorganization underlying bidirectional plasticity. *Nat Neurosci* 7(10):1104–1112.
45. Hadziselimovic N, et al. (2014) Forgetting is regulated via Musashi-mediated translational control of the Arp2/3 complex. *Cell* 156(6):1153–1166.
46. Thomas MJ, Malenka RC, Bonci A (2000) Modulation of long-term depression by dopamine in the mesolimbic system. *J Neurosci* 20(15):5581–5586.
47. Jeanes ZM, Buske TR, Morrisett RA (2011) In vivo chronic intermittent ethanol exposure reverses the polarity of synaptic plasticity in the nucleus accumbens shell. *J Pharmacol Exp Ther* 336(1):155–164.
48. Dunah AW, Standaert DG (2003) Subcellular segregation of distinct heteromeric NMDA glutamate receptors in the striatum. *J Neurochem* 85(4):935–943.
49. Thinschmidt JS, Walker DW, King MA (2003) Chronic ethanol treatment reduces the magnitude of hippocampal LTD in the adult rat. *Synapse* 48(4):189–197.
50. Zhang J, et al. (2009) PSD-95 uncouples dopamine-glutamate interaction in the D1/PSD-95/NMDA receptor complex. *J Neurosci* 29(9):2948–2960.
51. Kopec CD, Real E, Kessels HW, Malinow R (2007) GluR1 links structural and functional plasticity at excitatory synapses. *J Neurosci* 27(50):13706–13718.
52. Zhou Q, Homma KJ, Poo MM (2004) Shrinkage of dendritic spines associated with long-term depression of hippocampal synapses. *Neuron* 44(5):749–757.

53. Cuzon Carlson VC, et al. (2011) Synaptic and morphological neuroadaptations in the putamen associated with long-term, relapsing alcohol drinking in primates. *Neuropsychopharmacology* 36(12):2513–2528.
54. Marty VN, Spigelman I (2012) Long-lasting alterations in membrane properties, K(+) currents, and glutamatergic synaptic currents of nucleus accumbens medium spiny neurons in a rat model of alcohol dependence. *Front Neurosci* 6:86.
55. Isaac JTR, Ashby MC, McBain CJ (2007) The role of the GluR2 subunit in AMPA receptor function and synaptic plasticity. *Neuron* 54(6):859–871.
56. Nestler EJ (2001) Molecular basis of long-term plasticity underlying addiction. *Nat Rev Neurosci* 2(2):119–128.
57. Diana M, Tepper JM (2002) Electrophysiological pharmacology of mesencephalic dopaminergic neurons. *Handbook of Experimental Pharmacology II*, ed Di Chiara G (Springer, Berlin), Vol 154, pp 1–62.
58. Koob GF, Le Moal M (1997) Drug abuse: Hedonic homeostatic dysregulation. *Science* 278(5335):52–58.
59. Robinson TE, Berridge KC (2001) Incentive-sensitization and addiction. *Addiction* 96(1):103–114.
60. Weiss F, et al. (1996) Ethanol self-administration restores withdrawal-associated deficiencies in accumbal dopamine and 5-hydroxytryptamine release in dependent rats. *J Neurosci* 16(10):3474–3485.
61. Diana M, Pistis M, Muntoni A, Gessa G (1996) Mesolimbic dopaminergic reduction outlasts ethanol withdrawal syndrome: Evidence of protracted abstinence. *Neuroscience* 71(2):411–415.
62. Segal M, Andersen P (2000) Dendritic spines shaped by synaptic activity. *Curr Opin Neurobiol* 10(5):582–586.
63. Shepherd GM (1996) The dendritic spine: A multifunctional integrative unit. *J Neurophysiol* 75(6):2197–2210.
64. Uzbay IT, Kayaalp SO (1995) A modified liquid diet of chronic ethanol administration: Validation by ethanol withdrawal syndrome in rats. *Pharmacol Res* 31(1): 37–42.
65. Macey DJ, Schulteis G, Heinrichs SC, Koob GF (1996) Time-dependent quantifiable withdrawal from ethanol in the rat: Effect of method of dependence induction. *Alcohol* 13(2):163–170.
66. Smith AD, Bolam JP (1990) The neural network of the basal ganglia as revealed by the study of synaptic connections of identified neurones. *Trends Neurosci* 13(7):259–265.
67. Sanna E, et al. (2011) Voluntary ethanol consumption induced by social isolation reverses the increase of α(4)/δ GABA(A) receptor gene expression and function in the hippocampus of C57BL/6J mice. *Front Neurosci* 5:15.